Scalable expansion of iPSC and their derivatives across multiple lineages

Chee Keong Kwok [a,1], Isabelle Sébastien [b,1], Krithika Hariharan [b], Ina Meiser [c], Jeanette Wihan [b], Saskia Altmaier [c], Isabell Karnatz [b], Dominic Bauer [b], Benjamin Fischer [b], Alexander Feile [b], Alfredo Cabrera-Socorro [d], Mikkel Rasmussen [e], Bjørn Holst [e], Julia C. Neubauer [b,c], Christian Clausen [e], Catherine Verfaillie [f], Andreas Ebneth [d], Mattias Hansson [a], Rachel Steeg [g], Heiko Zimmermann [b,c,h,i,*]

[a] Cell Therapy R&D, Novo Nordisk A/S, Novo Nordisk Park 1, 2760 Måløv, Denmark
[b] Fraunhofer Project Center for Stem Cell Process Engineering, Fraunhofer Institute for Biomedical Engineering IBMT, Neunerplatz 2, 97082 Würzburg, Germany
[c] Fraunhofer Institute for Biomedical Engineering IBMT, Joseph-von-Fraunhofer-Weg 1, 66820 Sulzbach, Germany
[d] Neuroscience Therapeutic Area, Janssen Research & Development, Turnhoutseweg 30, 2340 Beerse, Belgium
[e] Bioneer A/S, Kogle Allé 2, 2970 Hørsholm, Denmark
[f] Department of Development and Regeneration, Stem Cell Institute, UZ Gasthuisberg, Herestraat 49, 3000 Leuven, Belgium
[g] Fraunhofer UK Research Ltd, Technology and Innovation Centre, 99 George Street, G1 1RD Glasgow, United Kingdom
[h] Department of Molecular and Cellular Biotechnology, Saarland University, 66123 Saarbrücken, Germany
[i] Facultad de Ciencias del Mar, Universidad Católica del Norte, Coquimbo, Chile

ARTICLE INFO

ABSTRACT

Induced pluripotent stem cell (iPSC) technology enabled the production of pluripotent stem cell lines from somatic cells from a range of known genetic backgrounds. Their ability to differentiate and generate a wide variety of cell types has resulted in their use for various biomedical applications, including toxicity testing. Many of these iPSC lines are now registered in databases and stored in biobanks such as the European Bank for induced pluripotent Stem Cells (EBiSC), which can streamline the quality control and distribution of these individual lines. To generate the quantities of cells for banking and applications like high-throughput toxicity screening, scalable and robust methods need to be developed to enable the large-scale production of iPSCs. 3D suspension culture platforms are increasingly being used by stem cell researchers, owing to a higher cell output in a smaller footprint, as well as simpler scaling by increasing culture volume. Here we describe our strategies for successful scalable production of iPSCs using a benchtop bioreactor and incubator for 3D suspension cultures, while maintaining quality attributes expected of high-quality iPSC lines. Additionally, to meet the increasing demand for "ready-to-use" cell types, we report recent work to establish robust, scalable differentiation protocols to cardiac, neural, and hepatic fate to enable EBiSC to increase available research tools.

1. Introduction

The discovery and development of human induced pluripotent stem cell (iPSC) technology [1,2] has been revolutionary for biomedical science. iPSCs can be derived from somatic cells of various genetic backgrounds and differentiated into cells of all the three germ layers. Similar to embryonic stem cells, iPSCs can be cultivated readily in the lab as they are self-renewing with unlimited proliferative capacity and can serve as a starting material for biomedical applications including toxicity studies, drug screening, disease modelling, as well as regenerative medicine [3]. Since this discovery, many iPSC lines have been generated by research groups all over the world, including control, disease-associated, as well as gene-edited cell lines. However, the high cost of generating and validating iPSC lines is a significant barrier to developing new iPSC lines. Therefore, there is a pressing need for cell banks of high-quality, validated iPSCs to serve as repositories to meet the various needs of the research and clinical communities. Indeed, both country/regional and international cell banking initiatives (e.g.

European Bank of induced Pluripotent Stem Cells (EBiSC), International Stem Cell Banking Initiative, hPSCreg, Global Alliance for iPSC Therapies) [4–10] have been established for these purposes. Additionally, large quantities of differentiated cells (e.g. cardiomyocytes, hepatocytes) may be required for high-throughput toxicity screening assays [11–13]. Moreover, iPSCs derived from the same or different donors may not behave similarly, even though they are well-characterised for pluripotency and reprogrammed by the same method. The sensitivity of cell lines to growth factors and inhibitors are often found to be different in practice, necessitating a titration of factors for every new cell line used for any published protocol. This demands robust and reliable protocols for upscaling the cultivation of undifferentiated iPSCs, as well as their subsequent differentiation into more terminally differentiated cell types.

To accomplish this, various approaches have been reported in the literature. A common method of culturing iPSCs at smaller scale is 2D adherent culture on plasticware (e.g. cell culture dishes, multi-well plates, T-flasks) coated with matrices such as Matrigel™, Geltrex™, vitronectin, laminins, or synthetic matrices such as Synthemax™ (reviewed in [14]). Multi-layer plasticware have been developed and are commercially available, such as Corning CellSTACK™ and Nunc Cell Factory™ [15]; these allow for increasing the amount of surface area for 2D adherent culture processes to achieve higher quantities of iPSCs. However, the use of multi-layer plasticware is labour-intensive and generates a high amount of plastic waste. Alternatively, automated 2D adherent culture systems, such as the CompacT SelecT™ platform [16], have also been shown to be a viable approach for the large-scale production of pluripotent stem cells. The drawbacks of this approach are the large initial capital investment of the equipment and the training of qualified personnel, as well as space requirements. Additionally, these 2D platforms rely on scaling out (i.e. increasing the number of vessels cultured in parallel) to produce the required cell quantities. Another type of adherent culture system is the hollow fibre bioreactor [17–19], where many capillary tubes are coated with matrix, then loaded with iPSCs. This provides a very large surface area for cells to attach to, while keeping a small physical footprint. However, in this system, cell growth is challenging to monitor during the expansion phase, and assessment can only be done at the point of harvesting. Additionally, owing to the narrow lumens of the capillaries, these systems are susceptible to clogging, leading to difficulties in ensuring that culture medium can be effectively distributed throughout the bioreactor, thereby resulting in the generation of nutrient/waste gradients, which may impact iPSC growth.

3D suspension culture platforms have been increasingly used for expansion of iPSCs, especially when high cell quantities are required, since these platforms are more easily scalable by increasing culture volume while maintaining the same cell density. Prior studies reported the expansion of embryonic stem cells on coated microcarriers kept in suspension in bioreactors [20–23]. These microcarriers can be made from a variety of materials such as polystyrene, glass, cellulose, or alginate [24,25] and coated with the same matrices used for 2D adherent cultures. When kept in suspension in a bioreactor, these microcarriers serve to increase the available surface area for cells to attach to by several fold [20,26]. After a period of cultivation, the cells can be dissociated from the microcarriers by chemical or enzymatic treatments. More recently, dissolvable microcarriers have been developed where the harvesting solution consists of several components, which dissociate cells from the microcarriers and simultaneously dissolve the microcarriers without negatively impacting cell viability [27]. After ROCK inhibition was found to promote the survival of dissociated embryonic stem cells [28], more studies have shown that embryonic stem cells and iPSCs can, without the need for surfaces to attach to, also be cultured and expanded in suspension as cell aggregates when treated with ROCK inhibitor (e.g. Y-27632) for the first 24–48 h of culture [29–36]. There are several 3D suspension platforms that have been tested with iPSCs with or without microcarriers. These include

stirred tank bioreactors [33,35,36], vertical wheel bioreactors [37,38], and rocking motion bioreactors [39].

Moreover, depending on the applications of the cells, several methods to expand and cryopreserve cells may be necessary. While passaging cells as single cells may afford more homogeneity and reproducibility in cell attachment, and in some applications may even be critical (e.g. single cell cloning for genome editing applications), passaging as single cells with ROCK inhibition has been linked to concerns surrounding genomic stability [40]. Some groups may even prefer to passage cells using non-enzymatic methods to dissociate cells as clumps rather than single cells. ROCK pathway modulation has also been suggested to influence downstream differentiation efficiencies [40,41], thereby warranting the development of protocols that offer the possibility of omitting ROCK inhibition during the undifferentiated cell expansion. Additionally, demands on cell quantities may vary widely; while 10^6 cells may be sufficient for lab scale activities, industrial scale manufacturing may require cell quantities several orders of magnitude higher than that. Therefore, the production of these cells needs to be flexible and scalable depending on a case-by-case basis. EBiSC is also aiming to provide not only undifferentiated iPSCs, but also differentiated cell types derived from a range of iPSC sources. Here, to meet the needs of the research community, EBiSC is uniquely positioned to couple the upscaled production of undifferentiated cells with their subsequent differentiation into more terminally differentiated cell types.

In this work, 3D experiments were performed in cell aggregate format or on Matrigel™-coated alginate microcarriers and in case of the neuronal differentiation compared to the standard 2D culture condition (planar culture, see Fig. 1). Expansion, differentiation, and cryopreservation processes were performed over multiple cell lines and towards different lineages. In all approaches, the suspension bioreactor system CERO 3D was used, as one optimised and flexible laboratory-scale device. The different workflow variations are represented in Fig. 2.

2. Materials and Methods

2.1. Cell lines

Five different EBiSC iPSC lines (IMI project, www.ebisc.org) were used, which are also registered on hpscreg.eu (Table 1). The EBiSC lines are fully consented for research use and quality controlled. At the point of banking with EBiSC, sterility (absence of mycoplasma, microbial growth), cell line identity based on short tandem repeat assay, as well as karyotyping are routinely performed; these data and accompanying Certificates of Analysis are available on request. Additionally, mycoplasma testing was performed on a regular basis. For the upscaling experiments the control lines UKBi005-A and BIONi010-C [42] were used, whereas the line BIONi010-C-13 [43] was chosen as gene-edited line with NGN2 transgene expression for neuronal differentiation. In case of the cardiac differentiation the control line UKBi005-A and the disease line UKKi018-A were used, and for the hepatic differentiation, a gene-edited daughter line from BIONi010-C-64 was used (edited with a CYP3A4-T2A-Nluc reporter, validated via genome sequencing). The cells were cultured on Matrigel™-coated cell culture dishes (MTG; Corning, USA) in mTeSR™1 medium (Stemcell Technologies, Canada) and split at 60–80% confluence with 0.5 mM ethylenediaminetetraacetic acid (EDTA) solution (Invitrogen, USA). Cell count and viability were determined on a NucleoCounter® NC-200™ device (ChemoMetec, Denmark).

2.2. 3D culture approaches

2.2.1. Culture as clumps

For seeded clumps (CL) in 3D, cells were previously detached from 2D culture with improved EDTA (iEDTA; proprietary formula based on EDTA, developed at Fraunhofer IBMT) after two DPBS (-/-) washing steps. As a culturing surface, Matrigel™-coated alginate microcarriers
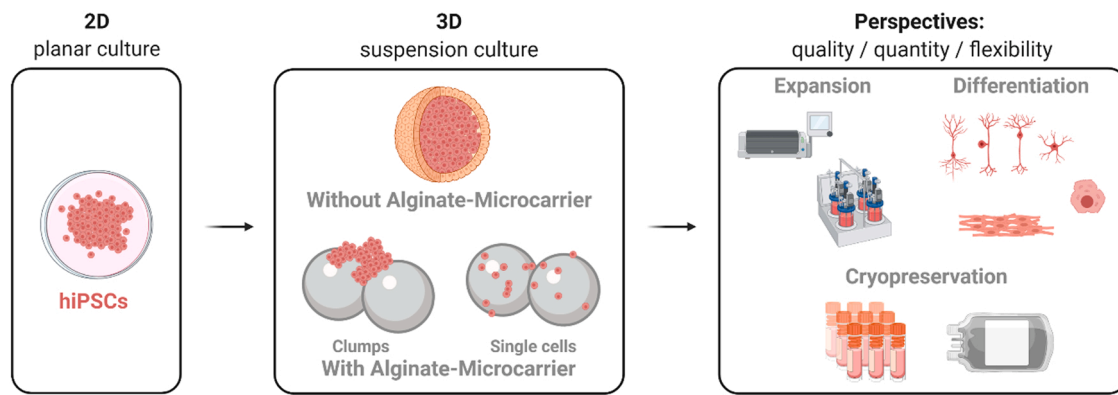
Fig. 1. Different approaches of the scalable expansion and differentiation of iPSCs with description of the culture formats used and resulting application fields.

(MC; Alginatec, Germany) of about 350 μm diameter were filtered and transferred together with the cells in a ratio of 60,000 cells per cm^2 to a CEROtube vessel (previously called LeviTube; OLS, Germany) designed for the bioreactor system CERO 3D (previously called BioLevitator; OLS, Germany). Culture conditions were 37 °C and 5% CO_2. The mixture of cells and beads was maintained in suspension through bi-directional rotation of the CEROtube (see Table 3 for details of Programme 1). After reaching confluence on the microcarriers, cells were incubated for about 20 min with iEDTA in the CERO 3D bioreactor at 60 rpm (Programme 2). Then the dissociation reaction was stopped with mTeSR™1 and the microcarriers removed from the cell suspension by straining them out using a 200 μm cell strainer (pluriSelect Life Science, Germany). Cells were centrifuged at 250 *g* for 3 min before further use (reseeding, quality control or banking).

2.2.2. Culture as single cells

Similar to the clumps protocol, iPSCs cultured as single cells (SC) on microcarrier were seeded in a ratio of 60,000 cells per cm^2 in CEROtubes and detached with iEDTA. Resuspension by pipetting was performed more intensively to reach a homogenous single cell suspension. mTeSR™1 medium was supplied with ROCK Inhibitor Y-27632 (Abcam, UK) in a final concentration of 10 μM. Programme 3 of the CERO device was used (Table 3).

With the aggregate protocols, iPSCs were washed with DPBS (-/-), then dissociated using TrypLE™ Select or Accutase® (Gibco, USA), resuspended in mTeSR™1 with 10 μM Y-27632 to stop dissociation, centrifuged at 300 *g* for 5 min, and resuspended in mTeSR™1 with 10 μM Y-27632. Thereafter, cells were seeded into CEROtubes. For the iPSC expansion as aggregates, 80 rpm rotation speed was chosen with a seeding density of 2×10^5 cells/ml (Programme 4, see Table 3). Aggregate dissociation was also performed at 80 rpm.

2.3. Cryopreservation procedure

Cells detached after the cardiac and neuronal differentiation were centrifuged at 250 *g* for 3 min and the pellet was resuspended in Cryo-Stor® CS10 (Stemcell Technologies, Canada) at a density of 8.5×10^6 cells per ml per cryovial (Greiner, Austria) for the neuronal differentiation (with the 3D aggregate condition) and 4–5×10^6 cells per ml per cryovial for the cardiac differentiation. Vials were then stored overnight at −80 °C in a freezing container (Mr. Frosty™) filled with sufficient isopropanol for gradual freezing (Thermo Fisher Scientific, Germany) and transferred during the next days to −150 °C liquid nitrogen cryogenic tanks in the vapour phase.

In brief, 5000–7000 hepatic organoids were slow frozen to −80 °C in vials at day 8 and 21 with 1 °C/min in 1 ml CryoStor® CS10 using the controlled rate freezer VIA Freeze (Cytiva). Subsequently, the vials were stored below −140 °C in liquid nitrogen tanks, thawed in 37 °C water bath, and further cultivated in a CERO 3D bioreactor. Details on the

cryopreservation results of the hepatic organoids produced as reported here, can be found in Altmaier et al. [44] in this issue.

2.4. Neuronal differentiation

For the neuronal differentiation triggered by NGN2 overexpression, the cell line BIONi010-C-13 was used [43]. Cells were dissociated with TrypLE™ Select and seeded as single cells for standard 2D, for aggregates, or on Matrigel™-coated alginate microcarriers (MC). Adapted from the iPSC culture protocols, a ratio of 60,000 cells per cm^2 growth surface was used with MC and 7.5×10^5 cells per ml seeding density for the aggregate approach, with respectively 40 and 60 rpm rotation speed in the CEROtubes (Programmes 3 and 5). In both cases, mTeSR™1 with 10 μM Y-27632 was needed in the first 24 h and replaced by mTeSR™1 alone on the following day. On day 2 of the experiments N2B27 medium (composition published by Shih et al. [45]) supplemented with 2 μg/ml doxycycline (DOX; Merck, USA) was used for two to five additional days to induce neuronal differentiation. At different harvest time points (day 0, day 2 and day 5), cells were washed with DPBS (-/-) and dissociated with Accutase® for 10 min at 60 rpm in the CERO 3D system (Programme 2 of Table 3). Cell count, immunocytochemistry and qPCR were performed.

2.5. Cardiac differentiation

Differentiation of iPSC cultures to early cardiomyocytes was based on the procedures according to Zhang et al. [46]. This protocol was adapted to function in three-dimensional conditions in suspension culture using CERO 3D bioreactors according to Fischer et al. [47]. To harvest iPSCs from dishes, the culture medium was aspirated, washed twice with 10 ml DPBS (-/-) and then treated with 6 ml TrypLE™ Select. After 5–7 min incubation at 37 °C, the enzymatic reaction was diluted with 6 ml mTeSR™1 and 10 μM Y-27632 and transferred to 50 ml centrifuge tubes (Greiner, Austria). After trituration, the cell count was determined using the NucleoCounter® NC-200™. Subsequently, the cells were centrifuged at 300 *g* for 3 min and seeded in cardiac differentiation medium in CEROtubes, set to 60 rpm rotation speed (Programme 5, Table 3). The cardiac differentiation medium is composed of a base medium, containing KnockOut™ DMEM (Thermo Fisher Scientific, USA) with Transferrin-Selenium (Sigma-Aldrich, USA), Glutamine (Thermo Fisher Scientific, USA), and Penicillin Streptomycin (Thermo Fisher Scientific, USA). The culture medium was changed every 24 h with addition of cardiac specific growth factors and inhibitors on day 0, day 2 and day 3 as listed in Table 2. On day 1, 4 and 7 the base media was used without additional growth factors. The standard and optimized protocol vary in growth factor and inhibitor concentrations as listed in Table 2. Dissociation of the spherical aggregates was performed by enzymatic digestion using papain (40 U/ml) (Worthington Biochemical, USA) mixed with 2 mM L-cysteine in DPBS (-/-) and incubated for at
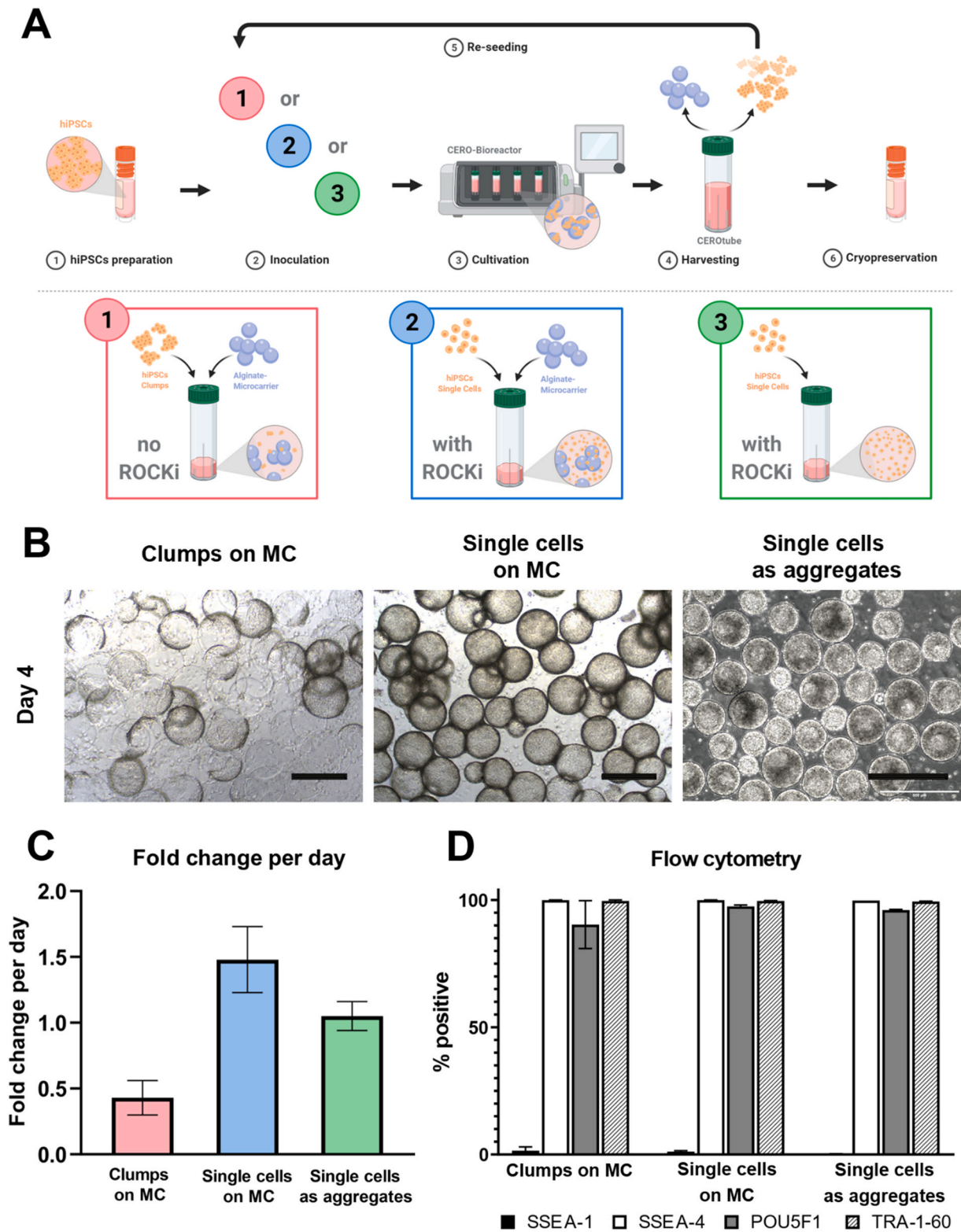
Fig. 2. Cultivation and expansion of iPSCs in 3D culture conditions. A: Workflow options of the 3D suspension cultivation. A1: iPSC clumps are seeded on Matrigel™-coated alginate microcarriers. A2: iPSC single cells are seeded on Matrigel™-coated alginate microcarriers in medium supplemented with 10 μM Y-27632. A3: iPSC single cell suspension forms aggregates with ROCK-inhibitor Y-27632 support. B: Morphology of the cells cultured as clumps and single cells on Matrigel™-coated alginate microcarriers (MC) and as aggregates. The cell line UKBi005-A was used for both microcarriers approaches and the cell line BIONi010-C for the aggregates approach. Scale bar = 500 μm. C: Graph representing the cell output potential of the three approaches with fold change in cells per day as parameter (n = 3). D: Flow cytometry analysis on the maintenance of the pluripotency-associated markers SSEA-4, TRA-1–60 and POU5F1 after harvest, with SSEA-1 included as a differentiation marker. Percentage of positive cells for these four markers are plotted (n = 3).

Table 1

EBiSC2 iPSC lines used for the expansion and differentiation experiments.

EBiSC cell line identifier	Descriptor	Reprogramming method	Donor Sex	BioSample ID
UKBi005-A	Healthy	Retrovirus	Female	SAMEA4584351
BIONi010-C	Healthy	Episomal	Male	SAMEA3158050
BIONi010-C-13	NGN2 induction	Episomal	Male	SAMEA103988285
UKKi018-A	Familial Long QT Syndrome	Sendai	Female	SAMEA17622418
BIONi010-C-64	CYP3A4-T2A- Nluc reporter	Episomal	Male	SAMEA10534760

Table 2

Concentration of factors used in cardiac differentiation.

Growth factor/ Inhibitor	Source	Standard Protocol	Optimised Protocol	Applied on
Activin A	Thermo Fisher Scientific, USA	10 ng/ml	20 ng/ml	Day 0
BMP4	Peprotech, USA	1 ng/ml	2 ng/ml	Day 0
FGF2	Peprotech, USA	10 ng/ml	10 ng/ml	Day 0
CHIR99021	Axon Medchem, Netherlands	1 µM	3 µM	Day 0
Wnt Inhibitor C59	Tocris Bioscience, UK	1 µM	2 µM	Day 2 and 3

least 20 min at 37 °C on day 8 of the suspension culture. Subsequently, the spheroids were incubated in a solution of base medium, KnockOut™ Serum Replacement (KO-SR) (Thermo Fisher Scientific, USA), 10 µM Y-27632 and 10 µM DNase (Sigma-Aldrich, USA). Enzyme action was blocked by washing with papain inhibitor E64 in the KO-SR containing base medium as well. After enzymatic dissociation, the isolated day 8 cardiomyocytes were cryopreserved as described before. Alternatively, single day 8 cells obtained from the spheroid dissociation were seeded on tissue culture flasks coated with recombinant laminins or fibronectin (in 2D) and cultivated for 1–2 weeks to enhance maturation. At day 16, cardiomyocytes are ready to be seeded on scaffolds and other materials to be tested, by day 25 they exhibit ideal electrophysiological properties and are used for pharmacological tests.

Cardiomyocytes were imaged using Nikon-Eclipse Ts2 microscope with phase contrast. Around 70–100 spheroids were examined on day 7 and day 8 at the end of the differentiation, before dissociation. The beat ratio for each sample is calculated by the following formula:

$$Amount\ of\ beating\ spheroids\ [\%] = \frac{Beating\ spheroids}{Total\ number\ of\ spheroids} \times 100$$

The amount of beating spheroids was calculated for cardiomyocytes generated from both UKBi005-A as well as UKKi018-A, as a readout of the efficiency of cardiac differentiation. Dissociated cardiomyocytes were also analysed by flow cytometry and qPCR.

2.6. Hepatic differentiation

The hepatic differentiation protocol was initially established in 2D based on protocols developed by Rezania et al. [48] towards definitive endoderm (DE), by Carpentier et al. [49] towards hepatic progenitor cells, and finally towards hepatocytes by Pettinato et al. [50]. The process then was translated to the suspension-based bioreactor CERO 3D. In pilot studies, process parameters were optimised to maximise homogeneity, biomass, and hepatocyte marker expression in 3D. Briefly, the rotation speed was set to 60 rpm without an inoculation phase and the medium viscosity was increased by the addition of 0.3% methylcellulose to slow down sedimentation and to prevent aggregation of the forming organoids. To start the differentiation protocol, iPSCs were harvested at a confluence of 70–80% as single cells using Accutase® (Gibco, USA): As soon as the colonies started to detach from the surface and appeared white in phase contrast microscopy, cells were rinsed in mTeSR™1 in the presence of 10 µM Y-27632 (Cayman Chemical Company, USA). Subsequently, 4×10^5 cells/ml, were inoculated in a total volume of 20 ml. The composition of the three differentiation media is described here in brief: Stage 1 medium (S1) to DE, consisted of KO-DMEM, 1% Pen/Strep/Glutamine, and Insulin-Transferrin-Selenium (all Fisher Scientific). Additional factors were 10 µM Y-27632 (Caymanchem), 1 µM CHIR99021 (Selleckchem), 10 ng/ml Activin A (Cell Guidance systems), 10 ng/ml Fibroblast Growth Factor-basic (Peprotech), 1 ng/ml Bone morphogenetic protein 4 (R&D), and 0.3% methylcellulose (R&D). For the second stage to hepatocyte progenitors, the medium consisted of DMEM/F12, 10% KOSR, 1% Glutamax, 1% Non-essential amino acids (NEAA), 1% Pen/Strep (all Fisher Scientific), 1% DMSO, and 0.3% methylcellulose (R&D). Medium was changed every second day. On day 3, medium was switched to William's E Medium without phenol red (Fisher Scientific) with Primary Hepatocyte Maintenance Kit (Fisher Scientific) and 0.5 µM Dexamethasone. Additionally, 50 ng/ml Recombinant Human Hepatocyte Growth Factor (Peprotech), and 30 ng/ml Recombinant Human Oncostatin M (Peprotech) were added. From days 17–24, 10 µM hydrocortisone (Selleckchem) and 1x cholesterol lipid concentrate (Gibco, 12531018) were added. Organoid size and count, metabolic analysis of functional hepatocyte marker CYP3A4 expression, cryopreservation, flow cytometry, immunocytochemistry and qPCR were performed and reported in Altmaier et al. [44]; key quantifications are presented in this article (Fig. 5). Further details on the hepatic differentiation in 2D and 3D and the cryopreservation approaches can be found in the report by Altmaier et al. [44] in this issue.

2.7. QC methods

2.7.1. Flow cytometry (FC)

Cell samples taken for flow cytometry analysis were washed twice with DPBS (-/-), fixed with 4% formaldehyde (Cytofix™; BD, USA) and stored at 4 °C after two washing steps with staining buffer (BD, USA) or DPBS (-/-). Before staining, cell samples were washed twice with Perm/Wash Buffer (BD, USA) and incubated for 10–15 min at room temperature. The cardiac samples were additionally incubated for 5 min in DPBS (+/+) supplemented with 1% FBS (Gibco, USA) at room temperature.

Table 3

CERO programmes used for 3D culture and differentiation of iPSCs. CL= clumps; MC = Matrigel™-coated alginate microcarriers; SC = single cells.

	Programme	Sub-programme	Rotation period [s]	Rotation speed [rpm]	Agitation period [min]	Agitation pause [min]	Duration [h]
1	**CL on MC culture**	Inoculation	4	40	2	15	5
		Cultivation	4	40	–	–	∞
2	**CL/SC on MC harvest**	Harvesting	5	60	–	–	∞
3	**SC on MC culture**	Inoculation	4	40	2	5	12
		Cultivation	4	40	–	–	∞
4	**SC culture + harvest**	Cultivation	4	80	–	–	∞
5	**SC differentiation**	Cultivation	2	60	–	–	∞

The Human and Mouse Pluripotent Stem Cell Analysis Kit (BD, USA) was used according to the manufacturer's instructions, with an additional antibody for staining of iPSC lines in the undifferentiated expansion approaches (see details in Table 4). Cardiac samples were stained with primary antibodies against Cardiac troponin and Ki-67, overnight at 4 °C followed by secondary antibody incubation for an hour at room temperature. The antibodies used are listed in Table 4.

Flow cytometry analysis has been performed in pilot studies for the hepatic differentiation to compare tested differentiation methods towards DE (FOXA2 and SOX17, data not shown). Details on these are included in the supplemental material in Altmaier et al. [44].

2.7.2. Immunocytochemistry (ICC)

2D ICC samples of the neuronal differentiations were washed twice with DPBS (+/+), fixed with 4% formaldehyde (Cytofix™. BD, USA) and stored at 4 °C after two washing steps with DPBS (+/+). After permeabilisation and blocking with 0.2% Triton™ X-100 (Merck, USA) and 1% BSA (Thermo Fisher Scientific, USA) in DPBS (+/+), primary antibodies were applied overnight at 4 °C. After three washing steps with 1% BSA in DPBS (+/+), cells were incubated for one hour with the secondary antibodies at room temperature and washed again three times with the identical solution. In the third washing step, DAPI was added (NucBlue™ Fixed Cell ReadyProbes™ Reagent, Invitrogen, USA) and replaced by DPBS (+/+) after 10 min.

2.7.3. Real time quantitative polymerase chain reaction (qPCR)

qPCR samples were lysed in RLT buffer (QIAGEN, Germany) and RNA was extracted using the RNeasy Plus Micro Kit (QIAGEN, Germany). After transcription to cDNA with the High-capacity cDNA Reverse Transcription Kit (Applied Biosystems, USA), qPCR analyses were pipetted in duplicates for the neuronal samples and in triplicates for the cardiac samples (see Table 5 for TaqMan assay list; Thermo Fisher Scientific, USA). Data was analysed with the Delta Delta Ct method and the relative quantification (RQ) or fold change in gene expression was plotted with iPSCs as reference sample (RQ = 1). *GAPDH* was used as an endogenous control.(Table. 6).

qPCR for the hepatic organoids using the markers HNF4A, AFP, TTR,

Table 4

List of antibodies (Ab) used for flow cytometry staining of hiPSC and cardiac cells.

Cells	Antibodies list	Dilution	Catalogue number
hiPSC	Alexa Fluor® 647 Rat anti-SSEA-4	20 µl per million cells	560477 (BD)
	PerCP-Cy™5.5 Mouse anti-Oct3/4		
	PE Rat anti-SSEA-1		
	Alexa Fluor® 647 Mouse IgG3, κ Isotype Control		
	PerCP-Cy™5.5 Mouse IgG1, κ Isotype Control		
	PE Mouse IgM, κ Isotype Control		
	Alexa Fluor® 488-conjugated anti-human TRA-1–60- R	5 µl per million cells	BLD-330614 (Biozol)
	Alexa Fluor® 488 Mouse IgM, κ Isotype Control	1.5 µl per million cells	BLD-401617 (Biozol)
Cardiac	Anti - cardiac troponin T (mouse monoclonal)	1:400	ab8295 (Abcam)
	Alexa Fluor® 488 goat anti-mouse	1:1000	A11001 (Thermo Fisher)
	Anti - Ki-67 (rabbit polyclonal)	1:400	ab15580 (Abcam)
	Alexa Fluor® 647 goat anti-rabbit	1:1000	A21236 (Thermo Fisher)
	Isotype mouse IgG1	1:200	M5284 (Sigma Aldrich)
	Isotype rabbit IgG	1:200	ab125938 (Abcam)

Table 5

List of antibodies (Ab) used for ICC staining of neuronal cells.

Antibodies list	Dilution	Catalogue number
Primary Ab1: Nestin	1:200	PA5–11887
Secondary Ab1: Goat anti Rabbit Alexa Fluor® 555	1:1000	A21429
Primary Ab2: Tubb3	1:1000	Ab7751
Secondary Ab2: Goat anti Rat Alexa Fluor® 488	1:1000	A11034
DAPI	2 drops per ml	R37606

ALB, CYP2C9, and CYP3A4 are not shown here but in Altmaier et al. [44].

3. Results

3.1. Implementation of 3D iPSC expansion approaches

For the comparison of the 3D iPSC expansion approaches, cells were cultured as clumps on Matrigel™-coated alginate microcarriers (MC), as aggregates from seeded single cell suspensions, as well as single cell (SC) suspensions on MC for at least one passage and up to four passages (clumps on MC and SC as aggregates). In terms of quantity, different cell attachment behaviour and proliferation of the cells was observed, as shown in the morphology pictures of Fig. 2B. With the "Clumps on MC" protocol (Fig. 2 A.1), UKBi005-A cells seeded as clumps showed lower cell adherence and more heterogeneous growth on the MC but did not require Y-27632 supplementation. This condition reached a fold change per day of 0.33 ± 0.19 (Fig. 2 C). With the protocol "SC on MC" (Fig. 2 A.2), single cells from the identical line were seeded on Matrigel™-coated alginate microcarriers and were observed to have the highest growth rates with a reached fold change per day of 1.48 ± 0.25 (confluency reached already after 3–4 days of cultivation). Microcarriers were almost completely covered with proliferating cells and the cells attached more homogeneously compared to the "Clump on MC" protocol. In case of the third protocol, "SC as aggregates" (Fig. 2 A.3), spherical aggregates with smooth, well-defined edges of approximately 220 µm diameter were obtained after 7 days of culture and reached a fold change per day of 1.07 ± 0.13 with the cell line BIONi010-C, representing a final harvest cell density of $1.52 \pm 0.19 \times 10^6$ cells/ml.

To assess cell quality, flow cytometry was performed on the three approaches (Clumps on MC, Single cells on MC, Single cells as aggregates) to observe the maintenance of the undifferentiated state at the final passage in 3D culture, by quantifying the presence of pluripotency-associated markers like SSEA-4, TRA-1–60, POU5F1, as well as SSEA-1 for differentiation. Across all three expansion conditions, cells were typically over 90% positive for pluripotency-associated markers, and below 5% positive for the differentiation marker SSEA-1 (Fig. 2D).

Table 6

List of TaqMan assays used for qPCR analyses:.

Target	TaqMan Assay ID
ACTN2	Hs00153809_m1
EOMES	Hs00172872_m1
GAPDH	Hs99999905_m1
ISL1	Hs00158126_m1
MAP2	Hs00258900_m1
MAPT	Hs00902194_m1
MESP1	Hs01001283_g1
MYH7	Hs01110632_m1
POU5F1	Hs00742896_s1
TNNT2	Hs00943911_m1
TUBB3	Hs00801390_s1

3.2. Fast and reproducible differentiation of iPSCs in (early) NGN2 induced neurons

With the NGN2-gene edited cell line BIONi010-C-13, the differentiation of iPSCs into early neurons was driven by short term doxycycline induction in N2B27. Following a pre-cultivation of two days in mTeSR™1, BIONi010-C-13 cells were characterised after 2 and 5 days of differentiation. They were cultivated in three different single cell culture formats: on 6 well plates (2D), on microcarrier (3D microcarrier) and as aggregates (3D aggregate) as shown in Fig. 3 A. Regarding the cell output potential, highest yield to day 0 was reached on day 5 by the 2D condition with a value of 9.9 ± 2.9, followed by the 3D microcarrier day 2 condition (Fig. 3B). Nevertheless, day 2 yields were quite similar across the three culture techniques and showed no significant

differences (2D: 7.0 ± 2.4, 3D aggregate: 8.1 ± 4.0, 3D microcarrier: 9.5 ± 5.1). The 3D aggregate and 3D microcarrier approaches performed well on day 5 under microscopic examination (pictures not shown) but the harvested cell amount permitted only yield of 2.1 and 1.5, as discussed later. Culturing of the parental BIONi010-C non-gene-edited line with N2B27 with doxycycline showed only signs of very early differentiation without the evident lineage specification that was seen with BIONi010-C-13 (data not shown).

At the different culture time points, qPCR was performed to characterise the maturity of the BIONi010-C-13 cells over the differentiation course. The expression profile of four markers showed clear similarity between the three cultivation approaches. Across all conditions, cells showed a profound downregulation of the pluripotent-associated marker *POU5F1* compared to iPSC with fold change values of up to
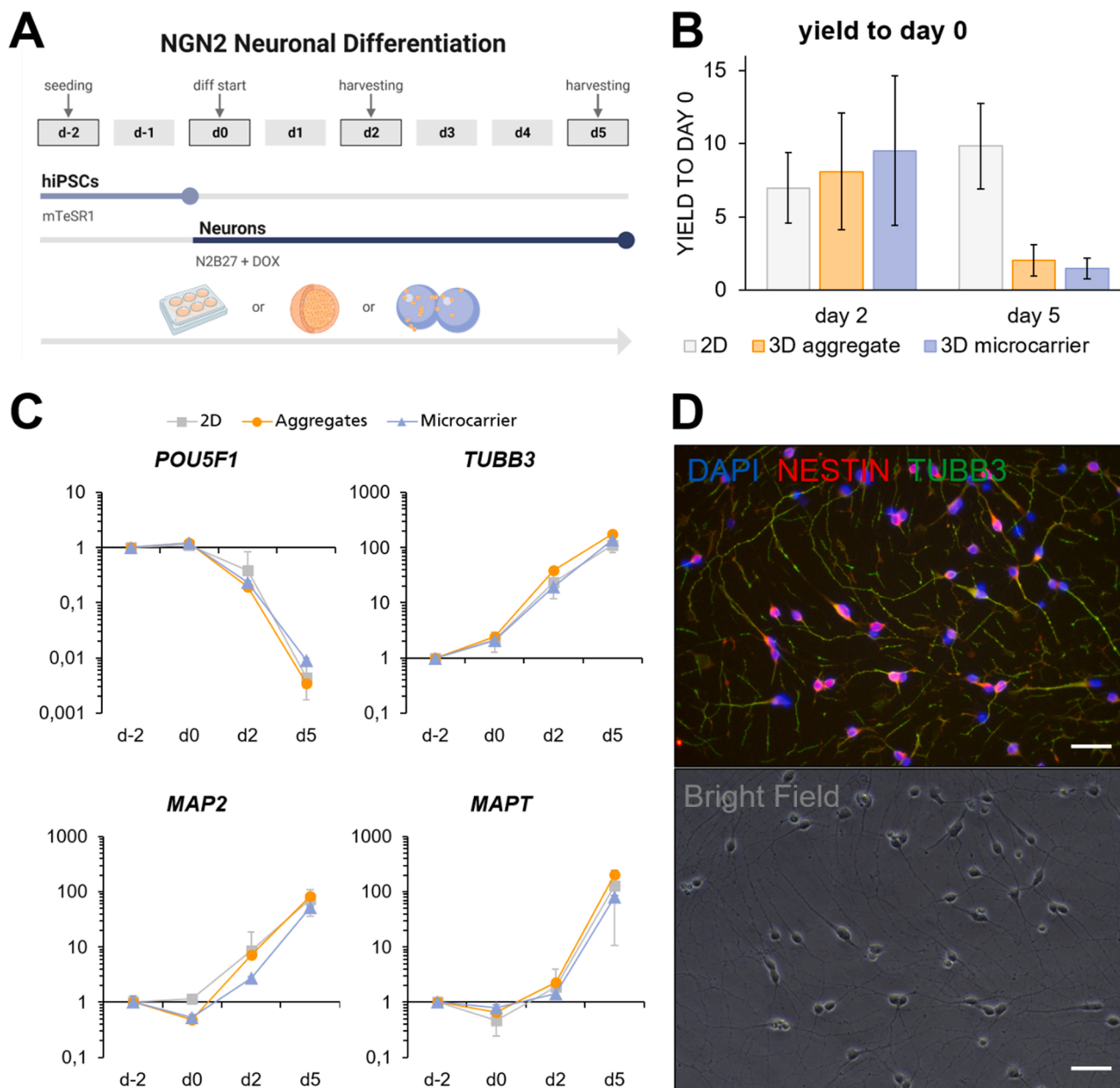
Fig. 3. Neuronal differentiation of iPSC in 2D, in 3D as aggregates and in 3D on Matrigel™-coated alginate microcarriers. A: Workflow of the differentiation protocol with details on the used media (mTeSR™1 and N2B27 +DOX) and the analysis time points (day −2, day 0, day 2 and day 5). B: Outgrowth potential of the differentiation with yield to day 0 plotted for the two harvest days of all three culture conditions (2D: n = 5; 3D aggregates: n = 5; 3D microcarrier: n = 3). C: qPCR analyses of the three conditions for four markers (POU5F1, TUBB3, MAP2, MAPT) with the relative quantification in gene expression to day 2 observed over time (2D: n = 5; 3D: n = 3). D: ICC and bright-field view of day 2 differentiated cells three days after thaw on a poly-L-ornithine (PLO)-laminin-coated plate. DAPI, Nestin and Tubb3 were used as staining markers. Fluorescence pictures have been merged and arranged with ImageJ. Scale bar = 100 μm.

900 times on day 5 for the microcarrier condition (Fig. 3 C). Conversely, the neuronal markers *TUBB3* and *MAP2* were expressed increasingly from day 2 on, while *MAPT*, as late stage marker, started to rise from day 5 on with fold change values to iPSC of 128, 204 and 81 for 2D, 3D aggregate and 3D microcarrier, respectively.

Based on these results, day 2 of the differentiation was chosen at the optimal time point for cryopreservation approaches with a recovery and viability of > 85% directly after thaw. It could be shown that cryopreserved cells recovered well and conserved their neuronal identity, as shown in Fig. 3D, where protein expressions of Tubb3 and Nestin was confirmed on a poly-L-ornithine (PLO)-laminin-coated well plate three days post thaw.

3.3. Optimised cardiomyocyte differentiation protocol increases reliability, robustness, and efficiency of cardiac cell generation across iPSC lines from diverse backgrounds

Cardiomyocytes were generated from iPSCs using a modified protocol from Zhang et al. [46], in the CERO 3D within eight days of culture. The protocol was modified previously to improve the yield of beating cardiac spheres in the healthy iPSC line UKBi005-A as well as the diseased iPSC line UKKi018-A (long QT syndrome, type 2-associated iPSC line). iPSCs were subjected to WNT activation (by addition of CHIR99021) in the presence of Activin A, BMP4 and FGF2 for 24 h followed by a WNT off phase effected by addition of a WNT inhibitor (Wnt-C59) for 48 h, crucial for the cardiac specification of iPSC (Fig. 4 A, growth factor concentrations listed in Table 2). Aggregates seeded on day 0 develop progressively into spheroids through the week of cardiac induction to form beating cardiac spheroids in the case of UKBi005-A (Fig. 4B). Initial trial of the standard protocol (SP) established for differentiation in the CERO 3D with the diseased UKKi018-A line (Fig. 4B) resulted in non-beating spheroids, necessitating an optimisation of the protocol. During the optimisation process, several aspects were investigated including the concentration of small molecule inhibitors and the temporal application of key pathway agonists / inhibitors important in cardiac lineage development. The optimised protocol (OP; growth factor concentrations listed in Table 2) is more robust across different iPSC lines; for example, UKKi018-A failed to generate beating spheroids with the standard differentiation protocol (n = 3) but with the optimised protocol robustly forms 86.2% beating spheroids by day 7 of differentiation (n = 2). Interestingly, this optimised protocol increases the percentage of beating spheroids generated from UKBi005-A from 63.5% up to 98.5% (n = 6 and n = 3, respectively) (Fig. 4 C). Such a detailed and robust optimisation is critical to allow efficient cardiomyocyte differentiation from many different iPSC lines without the need for cell line specific protocol alterations, which are cost and time consuming. The optimised protocol also greatly reduces variation in the number of beating spheroids generated (seen as reduced standard deviation bars). Another critical factor is generating high numbers of cardiomyocytes in a cost-efficient manner. Here, yield (i.e. the number of cardiomyocytes generated versus the number of iPSCs seeded) is consistently high at > 150%. These cardiomyocytes were assessed by flow cytometry to show around 98% cardiac troponin (cTNT) expression (Fig. 4E). A high co-expression of proliferation marker Ki-67 (Fig. 4E) indicates immaturity of these day 8 cardiomyocytes. Mature cardiomyocytes progressively lose their proliferative potential and show low levels of Ki-67. Gene expression also consistently shows a typical early cardiomyocyte identity with no elevated expression of mesodermal markers (*EOMES* and *MESP-1*). *ISL-1*, an early cardiomyocyte marker, is expressed at day 7 with low variability indicating a robust differentiation in the bioreactor (Fig. 4 F). Highly expressed are sarcomeric proteins (*ACTN2, MYH7* and *TNNT2*), which are essential for the cytoskeletal organisation and cardiac functionality.

3.4. Differentiation of iPSCs into hepatocyte-like cells

The differentiation protocol from iPSCs via definitive endoderm and hepatic progenitor cells to hepatocyte-like cells in 2D was successfully translated to the suspension bioreactor (see Fig. 5A) to form hepatic organoids. As shown in Fig. 5B, the forming aggregates became more compact and dense between day 3 and 4 days of the differentiation process in 3D. From day 4 onwards, their size slowly increases until the final differentiation day (day 21), coupled with a decrease in number of organoids over the same timeframe (Fig. 5C). Fig. 5D shows representative images of the morphological changes of the forming organoids along the cultivation period of 21 days.

3.5. Summary of expansion and differentiation capacity

In order to summarise the different proliferation potential of iPSC and differentiation capacities in the neuronal and cardiac lineages, we listed the number of harvested cells per 1 million seeded iPSCs for all approaches and formats. The results can be found in Table 7. We observed the highest output during the neuronal differentiation with a fold change of approximately 10 times within only 2 days, followed by the iPSC expansion in 2D and on MC with single cells within 7 days. While hepatic differentiation was accomplished in the CERO 3D, the aim was to generate intact hepatic organoids. Therefore, these organoids were not dissociated into single cells for cell counting. A comparison of the 2D and 3D hepatic differentiation approach is presented in Altmaier et al. [44].

4. Discussion

4.1. 3D expansion of undifferentiated iPSCs

Here we have shown that the upscaled expansion of iPSCs can be achieved using three different 3D approaches. The selection of an approach should ideally be informed by the aims of the investigator. Without ROCK inhibition, iPSC adherence to MCs may be low, particularly if the generated cell clumps are too small or if agitation rates are too high, resulting in growth- and adhesion-prohibitive shear stresses. Even when optimal-sized cell clumps are inoculated on MCs under adhesion-permissive agitation rates, cell clumps tend to attach to MCs heterogeneously. This does not impact on the possibility of undifferentiated cell expansion on MCs. However, this approach does require careful microscopic examination by trained and experienced operators to determine an optimal time-point for passaging to prevent excessive growth on MCs that may result in spontaneous differentiation or decrease cell viability. Another drawback of heterogeneous cell attachment may be the reproducibility or efficiency of downstream differentiation applications. Therefore, such an approach could be considered when ROCK inhibition severely affects downstream applications such as cell differentiation. Future development of this method could investigate the use of alternative chemical dissociation reagents that result in more homogeneously sized cell clumps, which are of sufficient size to attach to MCs quickly and efficiently.

By applying a single cell suspension and ROCK inhibition, cell attachment to MCs is more homogeneous and cell yields can be increased to a large extent compared to clumps (>3x fold). Additionally, coating of the MCs can be varied and adapted to individual needs and the culture format mimics the *in vivo* environment at its best. Alginate microcarriers could also be used to add further functionalities to optimise the workflow, e.g. controlled release of growth factors or smooth detachment of cells through switchable surfaces. A drawback of such an approach is the increase in number of handling steps to ensure cells adequately adhere to or detach from MCs. This can be overcome by culturing the cells as aggregates without the use of MCs. These aggregates can be formed easily and are relatively homogeneously sized, and aggregate size can be modulated by varying culture parameters, such as
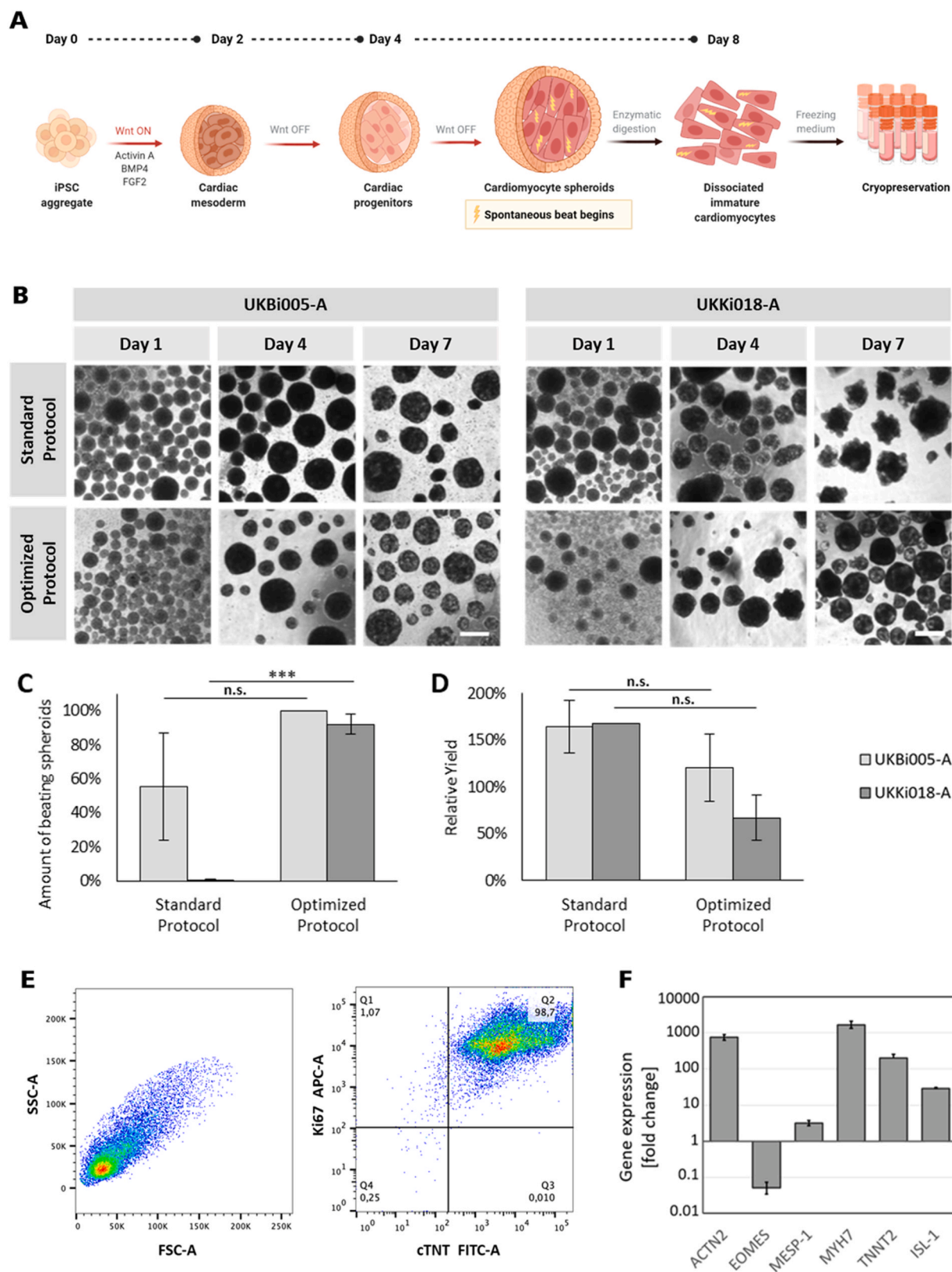
Fig. 4. Cardiac differentiation of iPSCs as 3D spheroids. A: Workflow of the cardiac differentiation from iPSCs up to cryopreservation of 8 days early cardiomyocytes. B: Morphology of spheroids from the two cell lines UKBi005-A and UKKi018-A over 7 days for the referenced (standard) and optimised protocol imaged by phase contrast microscopy (Scale bar: 500 μm). C: Percentage of beating spheroids for both cell lines and protocols (70–100 aggregates per replicate, performed in triplicates, n = 3 batches) (error bars represent SD). D: Cell output of the differentiation of both cell lines as relative yield in % (SP: n = 6 (UKBi005-A), n = 1 (UKKi018-A); OP: each n = 3). E: Flow cytometry analysis of the cardiac cells with cTNT/TNNT2 (cardiac marker) and Ki-67 (proliferation marker) for day 8 cells (n = 3). F: qPCR analysis of typical early Cardiomyocyte gene expression at day 7 of the line UKBi005-A for five specific markers (*ACTN2, EOMES, MESP-A, MYH7, TNNT2, ISL-1*) (n = 3) data given as fold change compared to iPSCs at the d0; error bars represent 95% confidence intervals.
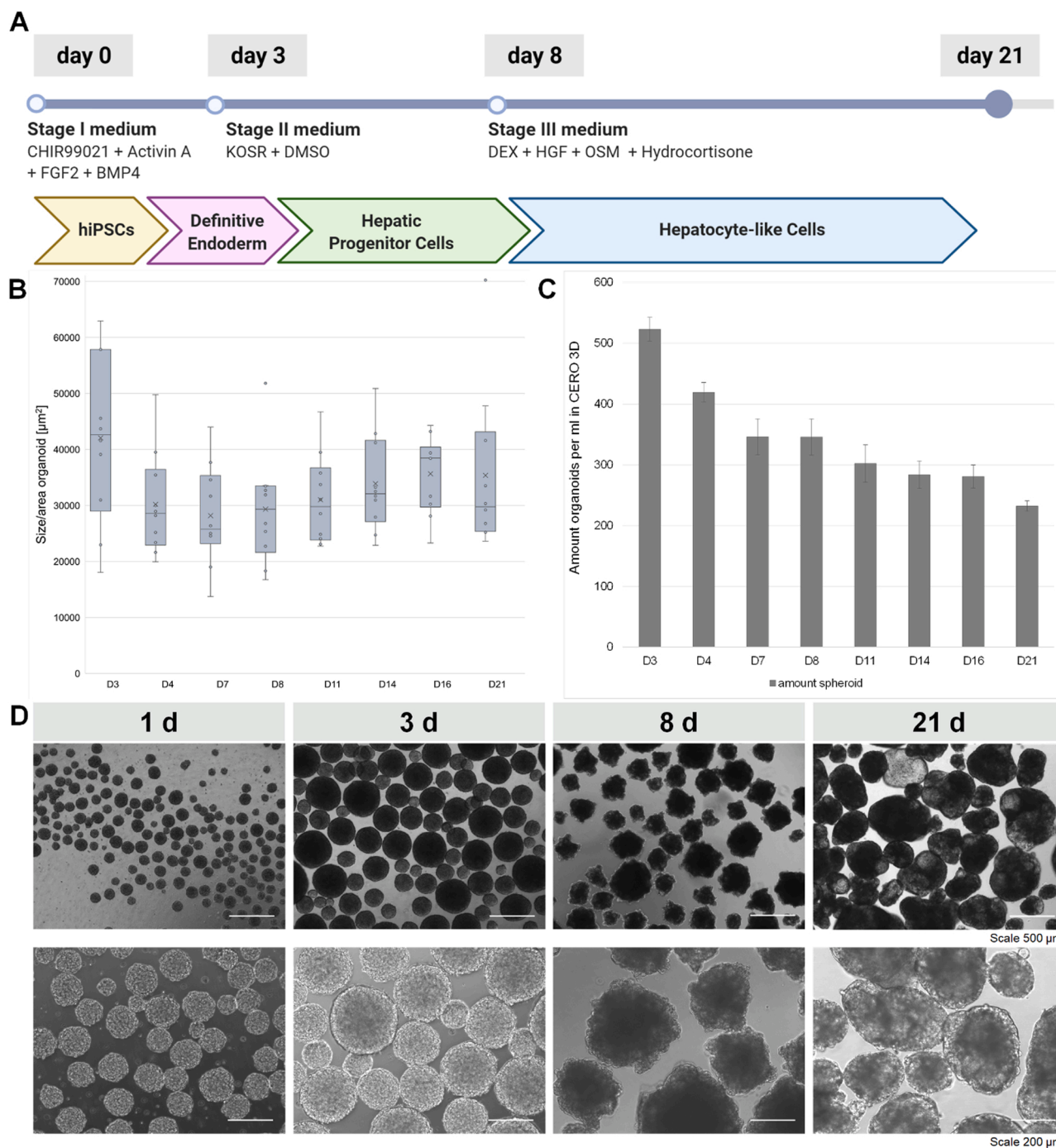
Fig. 5. A: Schematic overview of the differentiation protocol from iPSCs to hepatocyte-like cells. B: Development of the organoid size throughout the differentiation (n = 3). C: Number of organoids produced in 20 ml (n = 3). D: Representative microscopic images during the development of hepatic organoids.

cell seeding densities and agitation rates. High reproducibility and ease of handling were outstanding in this approach. When such approaches involving ROCK inhibition are used, the high number of surviving cells results in a faster culture period until they are ready to harvest. However, there is a risk of accumulating genomic aberrations as cells are pushed to survive even in the stressful single cell state. Care should therefore be taken to ensure that cells do not overgrow MCs, or that cell aggregates do not exceed a certain size whereby nutrient and gas diffusion limits can adversely affect growth and viability of cell aggregates. Once such limits have been determined, they can be used to define end-points of a culture period, where cells can then be applied in other downstream processes such as differentiation or dissociated for

cryopreservation and banking. Scalable workflows of iPSC expansion as presented here produce enough cells for e.g. toxicological screening (see output capacity in Table 7).

4.2. Neuronal differentiation

Besides iPSC expansion, we evaluated the upscaling capacity of the neuronal differentiation with doxycycline induction of NGN2-edited iPSC lines (Fig. 3B). Compared to conventional growth-factor based differentiation approaches (e.g. dual SMAD inhibition [51–53]), the overexpression of the lineage-determining transcription factor NGN2 allows an accelerated differentiation and yields a more homogenous and

Table 7
Output capacity during iPSC expansion and differentiation from 1×10^6 cells seeding:.

Cell type	Seeded cells	2D	3D on MC	3D as aggregates
iPSC expansion (7 days later)	Clumps	5.9×10^6	2.3×10^6	–
	Single Cells	1.0×10^7	1.0×10^7	7.6×10^6
iPSC-derived neurons (2 days later)	Single Cells	7.0×10^6	8.1×10^6	9.5×10^6
iPSC-derived cardiomyocytes (7 days later)	Single Cells	–	–	UKBi005-A: 1.5×10^6 UKKi018-A: 8.7×10^5

reproducible population [45] after only two days of differentiation in a 2D condition as well as in 3D (with and without MC). Proliferation in 2D cultures continued until day 5, even though to a lower extent, as cells started to get post-mitotic. A similar increase in the cell amount was present in 3D conditions. Here, we observed a growing diameter of aggregates and an increased cell confluence on microcarriers. However, the cells could not be detached from the MCs or dissociated from the aggregates properly to reach a single cell suspension resulting in underestimated cell counts. Although not yet investigated, we presume that the strength of intercellular contacts in 3D approaches exceeds the physical interactions in planar 2D cultures. A stronger mechanical detachment of the cells or the use of reagents like the EB dissociation Kit (Miltenyi Biotec, Germany) may represent a suitable alternative, but harsh dissociation conditions might affect the viability of the cells, their integrity and re-attachment capacity. Although high standard deviations in cell count were observed across all conditions, both qPCR analyses on day 2 and day 5, as well as ICC staining three days post-thaw confirmed a reproducible differentiation of iPSC into neurons that express classical lineage-specific markers such as TUBB3, MAP2 and MAPT (Fig. 3C and D). Overall, the differentiation efficiency in 3D approaches was undistinguishable from 2D cultures highlighting the potential of our 3D protocols for a large-scale production of neurons. Besides the better medium/volume ratio and mimicking of the *in vivo* environment, 3D culture on MCs also takes the advantage of a cell-matrix interaction and has flexibility in how the growth surface can be coated.

With the translation of the 2D neuronal differentiation protocol to the 3D culture format in laboratory scale, we could reach an important milestone in the production of high quantities of good quality, iPSC-derived neuronal cells for toxicity, functionality, and more complex model testing.

4.3. Cardiac differentiation

Differentiating iPSCs to cardiomyocytes has been accomplished by several labs. Nevertheless, the challenge of using a single protocol for several iPSC lines, healthy as well as diseased, requires a titration of factors for every new cell line used for any published protocol. This study compares a standard protocol adapted from Fischer et al. [47] with an optimised protocol that triggers differentiation in a non-responding disease-associated cell line. The optimised protocol enables generation of cardiomyocytes from 'hard to differentiate' iPSC lines in addition to increasing beating spheroid generation in cell lines that respond well to the standard protocol. This potentiates the application of this optimised protocol to develop and distribute cardiomyocyte products from many donors in a rapid and cost-efficient manner, supporting goals for sustainability. A direct upscale of iPSCs to cardiomyocytes was observed only in the healthy cell line (UKBi005-A) with at least a 1.5-fold increase (Table 7) in cell quantity compared to the number of input iPSCs. With the standard protocol, both the healthy and the disease-associated cell line (UKKi018-A) resulted in similar total

cell quantities but with a clear difference in the proportion of beating spheroids; interestingly, with the optimised protocol, while both cell lines showed a reduction in cell yield compared to the standard protocol, the proportion of beating spheroids was increased dramatically in both cell lines. Further cell lines are being tested for their performance with the optimised protocol. The cardiomyocytes obtained at day 8 have several desirable features including high cTNT expression, early mRNA detection of specific cardiac cytoskeletal markers, spontaneous beating and high proliferative capacity. This deems them immature, yet their rapid proliferation facilitates their upscaling at the cardiomyocyte level, fuelling efforts for large-scale production of a more mature cardiomyocyte population. Day 8 early cardiomyocytes recover quickly after thawing and can be grown on tissue culture surfaces coated with laminin or fibronectin (Supplementary figure 1). On day 8, cardiomyocytes cannot be tested for electrophysiological properties as spheroids, hence they are cultivated further. For future further functional characterisation of these cardiomyocytes, recordings of their field potential duration could be measured after a week of culture on micro-electrode arrays. A week or two after 2D cultivation, mature cardiomyocytes suitable for functional assays and toxicity testing may be obtained. On day 25, mature electrophysiologically stable cardiomyocytes could also be subjected to compounds from the CiPA study [54], to evaluate the presence of all ion channels required for functionality.

4.4. Hepatic differentiation

The iPSC-derived hepatocyte-like cells have the potential to serve as an alternative source for primary human hepatocytes (PHH). PHHs have been successfully applied as *in vitro* models e.g. for the assessment of hepatotoxicity, but their number is limited and they exhibit a narrow application window due to poor performance in lab conditions. In contrast, iPSC-derived hepatic cells differentiated and cultivated as three-dimensional multicellular aggregates cope well in culture and often show an improved hepatic phenotype because the physiological environment is mimicked [55]. We show here that the generation of hepatic organoids in scalable suspension-based bioreactors is possible from iPSCs via definitive endoderm to hepatocyte-like cells after 21 days of differentiation. As the microscopic images of the developing hepatic organoids show (Fig. 5D), their level of compactness changes throughout the cultivation process. This addresses the discrepancy between a minor increase in organoid size after day 8 of differentiation (Fig. 5B) and the reduced number of the organoids generated (Fig. 5C). Most likely, the morphological change is caused by the transition from stage 2 to stage 3 medium, when the cells further mature and switch from the hepatic progenitor to the hepatocyte-like state. Since the strength of intracellular contacts in an organoid quickly increase along the hepatic maturation, their dissociation and thus the assessment of yield on single cell basis is not applicable. The decrease in organoid number along the differentiation and maturation process is most likely caused by aggregation of two or more organoids. In order to avoid such aggregation and to more tightly control the organoid size, an increase of the rotation speed with size progression is indicated. The influence of resulting increased shear force to the functionality of hepatic organoids needs to be evaluated in further studies. The functionality of the produced organoids has been assessed via metabolic activity, as well as immunocytochemical staining and qPCR analysis of relevant hepatic markers. Data can be seen in the article Altmaier et al. [44] in this journal's issue. The strength of this reported hepatic organoid production lies in the more physiological three-dimensional character to promote cell's functionality (e.g. CYP3A4 expression) and the potential of scalability of the cultivation technique by parallelisation to meet the increasing numbers requested in biomedical research.

5. Conclusions

In this paper, we have presented the establishment and optimisation of different expansion and differentiation protocols starting from several different iPSC lines. These iPSC lines are catalogued and made available through the European Bank for induced pluripotent Stem Cells (EBiSC). All approaches were performed in the identical bioreactor system, showing the flexibility and adaptability of the device for individual needs, as well as providing insights into approaches for upscaling the production of undifferentiated and differentiated cells in such 3D culture formats. High quantities of iPSCs and iPSC-derived progeny (up to 10x fold change) could be harvested and matured in these 3D culture formats, thereby demonstrating the feasibility of using these robust protocols to reproducibly generate a variety of cell types for toxicity screening and compound testing.

Declaration of Competing Interest

The authors declare the following financial interests/personal relationships which may be considered as potential competing interests: Chee Keong Kwok reports a relationship with Novo Nordisk A/S that includes: employment. Alfredo Cabrera-Socorro reports a relationship with Janssen Pharmaceutica NV that includes: employment. Mattias Hansson reports a relationship with Novo Nordisk A/S that includes: employment and equity or stocks.

Appendix A. Supporting information

Supplementary data associated with this article can be found in the online version at doi:10.1016/j.reprotox.2022.05.007.

References

[1] K. Takahashi, K. Tanabe, M. Ohnuki, M. Narita, T. Ichisaka, K. Tomoda, S. Yamanaka, Induction of pluripotent stem cells from adult human fibroblasts by defined factors, Cell 131 (2007) 861–872, https://doi.org/10.1016/j.cell.2007.11.019.

[2] J. Yu, M.A. Vodyanik, K. Smuga-Otto, J. Antosiewicz-Bourget, J.L. Frane, S. Tian, J. Nie, G.A. Jonsdottir, V. Ruotti, R. Stewart, I.I. Slukvin, J.A. Thomson, Induced pluripotent stem cell lines derived from human somatic cells, Science 318 (2007) 1917–1920, https://doi.org/10.1126/science.1151526.

[3] Y. Shi, H. Inoue, J.C. Wu, S. Yamanaka, Induced pluripotent stem cell technology: a decade of progress, Nat. Rev. Drug Discov. 16 (2016) 115, https://doi.org/10.1038/nrd.2016.245.

[4] M. Turner, S. Leslie, N.G. Martin, M. Peschanski, M. Rao, C.J. Taylor, A. Trounson, D. Turner, S. Yamanaka, I. Wilmut, Toward the development of a global induced pluripotent stem cell library, Cell Stem Cell 13 (2013) 382–384, https://doi.org/10.1016/j.stem.2013.08.003.

[5] G.N. Stacey, L. Healy, The International Stem Cell Banking Initiative (ISCBI), Stem Cell Res. 53 (2021), 102265, https://doi.org/10.1016/J.SCR.2021.102265.

[6] S. Sullivan, P. Ginty, D. McMahon, M. May, S.L. Solomon, A. Kurtz, G.N. Stacey, A. Bennaceur Griscelli, R.A. Li, J. Barry, J. Song, M.L. Turner, The Global Alliance for iPSC Therapies (GAiT), Stem Cell Res. 49 (2020), 102036, https://doi.org/10.1016/J.SCR.2020.102036.

[7] A. Kurtz, G. Stacey, L. Kidane, A. Seriola, H. Stachelscheid, A. Veiga, Regulatory insight into the European human pluripotent stem cell registry, Stem Cells Dev. 23 (2014) 51–55, https://doi.org/10.1089/scd.2014.0319.

[8] N. Mah, S. Seltmann, B. Aran, R. Steeg, J. Dewender, N. Bultjer, A. Veiga, G. N. Stacey, A. Kurtz, Access to stem cell data and registration of pluripotent cell lines: the human pluripotent stem cell registry (hPSCreg), Stem Cell Res. 47 (2020), 101887, https://doi.org/10.1016/j.scr.2020.101887.

[9] R. Steeg, J.C. Neubauer, S.C. Müller, A. Ebneth, H. Zimmermann, The EBiSC iPSC bank for disease studies, Stem Cell Res. 49 (2020), 102034, https://doi.org/10.1016/j.scr.2020.102034.

[10] T. Hanatani, N. Takasu, CiRA iPSC seed stocks (CiRA's iPSC Stock Project), Stem Cell Res. 50 (2021), 102033, https://doi.org/10.1016/j.scr.2020.102033.

[11] F.A. Grimm, Y. Iwata, O. Sirenko, M. Bittner, I. Rusyn, High-content assay multiplexing for toxicity screening in induced pluripotent stem cell-derived cardiomyocytes and hepatocytes, ASSAY Drug Dev. Technol. 13 (2015) 529–546, https://doi.org/10.1089/adt.2015.659.

[12] G. Witt, O. Keminer, J. Leu, R. Tandon, I. Meiser, A. Willing, I. Winschel, J.-C. Abt, B. Brändl, I. Sébastien, M.A. Friese, F.-J. Müller, J.C. Neubauer, C. Claussen, H. Zimmermann, P. Gribbon, O. Pless, An automated and high-throughput-screening compatible pluripotent stem cell-based test platform for developmental and reproductive toxicity assessment of small molecule compounds, Cell Biol. Toxicol. 2 (37) (2020) 229–243, https://doi.org/10.1007/S10565-020-09538-0.

[13] J.C. del Álamo, D. Lemons, R. Serrano, A. Savchenko, F. Cerignoli, R. Bodmer, M. Mercola, High throughput physiological screening of iPSC-derived cardiomyocytes for drug development, Biochim. Et Biophys. Acta (BBA) - Mol. Cell Res. 1863 (2016) 1717–1727, https://doi.org/10.1016/J.BBAMCR.2016.03.003.

[14] L.G. Villa-Diaz, A.M. Ross, J. Lahann, P.H. Krebsbach, Concise review: The evolution of human pluripotent stem cell culture: from feeder cells to synthetic coatings, Stem Cells 31 (2013) 1–7, https://doi.org/10.1002/stem.1260.

[15] S. Tohyama, J. Fujita, C. Fujita, M. Yamaguchi, S. Kanaami, R. Ohno, K. Sakamoto, M. Kodama, J. Kurokawa, H. Kanazawa, T. Seki, Y. Kishino, M. Okada, K. Nakajima, S. Tanosaki, S. Someya, A. Hirano, S. Kawaguchi, E. Kobayashi, K. Fukuda, Efficient large-scale 2D culture system for human induced pluripotent stem cells and differentiated cardiomyocytes, Stem Cell Rep. 9 (2017) 1406–1414, https://doi.org/10.1016/J.STEMCR.2017.08.025.

[16] R.J. Thomas, D. Anderson, A. Chandra, N.M. Smith, L.E. Young, D. Williams, C. Denning, Automated, scalable culture of human embryonic stem cells in feeder-free conditions, Biotechnol. Bioeng. 102 (2008) 1636–1644, https://doi.org/10.1002/bit.22187.

[17] C. Gerlach, E. Schmelzer, Multicompartmental hollow-fiber-based bioreactors for dynamic three-dimensional perfusion culture, Methods Mol. Biol. (2016), https://doi.org/10.1007/7651.

[18] F.C. Paccola Mesquita, C. Hochman-Mendez, J. Morrissey, L.C. Sampaio, D. A. Taylor, Laminin as a potent substrate for large-scale expansion of human induced pluripotent stem cells in a closed cell expansion system, Stem Cells Int. (2019), https://doi.org/10.1155/2019/9704945.

[19] K. Ikeda, S. Nagata, T. Okitsu, S. Takeuchi, Cell fiber-based three-dimensional culture system for highly efficient expansion of human pluripotent stem cells, Sci. Rep. 7 (2017) 1–10, https://doi.org/10.1038/s41598-017-03246-2.

[20] A.K. Chen, X. Chen, A.B.H. Choo, S. Reuveny, S.K.W. Oh, Expansion of Human Embryonic Stem Cells on Cellulose Microcarriers, in: Current Protocols in Stem Cell Biology, John Wiley & Sons, Ltd, 2010: pp. 1C.11.1–1C.11.14. https://doi.org/10.1002/9780470151808.sc01c11s14.

[21] B.W. Phillips, R. Horne, T.S. Lay, W.L. Rust, T.T. Teck, J.M. Crook, Attachment and growth of human embryonic stem cells on microcarriers, J. Biotechnol. 138 (2008) 24–32, https://doi.org/10.1016/j.jbiotec.2008.07.1997.

[22] S.K.W. Oh, A.K. Chen, Y. Mok, X. Chen, U.M. Lim, A. Chin, A.B.H. Choo, S. Reuveny, Long-term microcarrier suspension cultures of human embryonic stem cells, Stem Cell Res. 2 (2009) 219–230, https://doi.org/10.1016/j.scr.2009.02.005.

[23] L.T. Lock, E.S. Tzanakakis, Expansion and differentiation of human embryonic stem cells to endoderm progeny in a microcarrier stirred-suspension culture, Tissue Eng. Part A 15 (2009) 2051–2063, https://doi.org/10.1089/ten.tea.2008.0455.

[24] M.M. Gepp, B. Fischer, A. Schulz, J. Dobringer, L. Gentile, J.A. Vásquez, J. C. Neubauer, H. Zimmermann, Bioactive surfaces from seaweed-derived alginates for the cultivation of human stem cells, J. Appl. Phycol 5 (29) (2017) 2451–2461, https://doi.org/10.1007/S10811-017-1130-6.

[25] A.K.-L. Chen, S. Reuveny, S.K.W. Oh, Application of human mesenchymal and pluripotent stem cell microcarrier cultures in cellular therapy, Biotechnol. Adv. 31 (2013) 1032–1046, https://doi.org/10.1016/j.biotechadv.2013.03.006.

[26] D.E. Kehoe, D. Jing, L.T. Lock, E.S. Tzanakakis, Scalable stirred-suspension bioreactor culture of human pluripotent stem cells, Tissue Eng. Part A 16 (2010) 405–421, https://doi.org/10.1089/ten.tea.2009.0454.

[27] A.L. Rodrigues, C.A.V. Rodrigues, A.R. Gomes, S.F. Vieira, S.M. Badenes, M. M. Diogo, J.M.S. Cabral, Dissolvable microcarriers allow scalable expansion and harvesting of human induced pluripotent stem cells under xeno-free conditions, Biotechnol. J. (2018) 1800461, https://doi.org/10.1002/biot.201800461.

[28] K. Watanabe, M. Ueno, D. Kamiya, A. Nishiyama, M. Matsumura, T. Wataya, J. B. Takahashi, S. Nishikawa, S. Nishikawa, K. Muguruma, Y. Sasai, A ROCK inhibitor permits survival of dissociated human embryonic stem cells, Nat. Biotechnol. 25 (2007) 681–686, https://doi.org/10.1038/nbt1310.

[29] R. Zweigerdt, Large Scale Production of Stem Cells and Their Derivatives, in: U. Martin (Ed.), Engineering of Stem Cells, Springer, Berlin, Heidelberg, Germany, 2009: pp. 201–235. https://doi.org/10.1007/10_2008_27.

[30] R. Zweigerdt, R. Olmer, H. Singh, A. Haverich, U. Martin, Scalable expansion of human pluripotent stem cells in suspension culture, Nat. Protoc. 6 (2011) 689–700, https://doi.org/10.1038/nprot.2011.318.

[31] H. Singh, P. Mok, T. Balakrishnan, S.N.B. Rahmat, R. Zweigerdt, Up-scaling single cell-inoculated suspension culture of human embryonic stem cells, Stem Cell Res. 4 (2010) 165–179, https://doi.org/10.1016/J.SCR.2010.03.001.

[32] R. Olmer, A. Lange, S. Selzer, C. Kasper, A. Haverich, U. Martin, R. Zweigerdt, Suspension culture of human pluripotent stem cells in controlled, stirred bioreactors, Tissue Eng. Part C: Methods 18 (2012) 772–784, https://doi.org/10.1089/ten.tec.2011.0717.

[33] C. Kropp, H. Kempf, C. Halloin, D. Robles-Diaz, A. Franke, T. Scheper, K. Kinast, T. Knorpp, T.O. Joos, A. Haverich, U. Martin, R. Zweigerdt, R. Olmer, Impact of feeding strategies on the scalable expansion of human pluripotent stem cells in single-use stirred tank bioreactors, Stem Cells Transl. Med. 5 (2016) 1289–1301, https://doi.org/10.5966/sctm.2015-0253.

[34] A. Elanzew, A. Sommer, A. Pusch-Klein, O. Brüstle, S. Haupt, A reproducible and versatile system for the dynamic expansion of human pluripotent stem cells in suspension, Biotechnol. J. 10 (2015) 1589–1599, https://doi.org/10.1002/biot.201400757.

[35] C.K. Kwok, Y. Ueda, A. Kadari, K. Günther, S. Ergün, A. Heron, A.C. Schnitzler, M. Rook, F. Edenhofer, Scalable stirred suspension culture for the generation of billions of human induced pluripotent stem cells using single-use bioreactors, J. Tissue Eng. Regen. Med. 12 (2018) e1076–e1087, https://doi.org/10.1002/term.2435.

[36] F. Manstein, K. Ullmann, C. Kropp, C. Halloin, W. Triebert, A. Franke, C.M. Farr, A. Sahabian, A. Haase, Y. Breitkreuz, M. Peitz, O. Brüstle, S. Kalies, U. Martin, R. Olmer, R. Zweigerdt, High density bioprocessing of human pluripotent stem cells by metabolic control and in silico modeling, Stem Cells Transl. Med. (2021) 1063–1080, https://doi.org/10.1002/sctm.20-0453.

[37] B.S. Borys, T. Dang, T. So, L. Rohani, T. Revay, T. Walsh, M. Thompson, B. Argiropoulos, D.E. Rancourt, S. Jung, Y. Hashimura, B. Lee, M.S. Kallos, Overcoming bioprocess bottlenecks in the large-scale expansion of high-quality hiPSC aggregates in vertical-wheel stirred suspension bioreactors, Stem Cell Res. Ther. 2021 12 1 (12) (2021) 1–19, https://doi.org/10.1186/S13287-020-02109-4.

[38] C.A. Rodrigues, T.P. Silva, D.E. Nogueira, T.G. Fernandes, Y. Hashimura, R. Wesselschmidt, M.M. Diogo, B. Lee, J.M. Cabral, Scalable culture of human induced pluripotent cells on microcarriers under xeno-free conditions using single-use vertical-wheelTM bioreactors, J. Chem. Technol. Biotechnol. 93 (2018) 3597–3606, https://doi.org/10.1002/JCTB.5738.

[39] B.M. Davis, E.R. Loghin, K.R. Conway, X. Zhang, Automated closed-system expansion of pluripotent stem cell aggregates in a rocking-motion bioreactor, Slas Technol.: Transl. Life Sci. Innov. 23 (2018) 364–373, https://doi.org/10.1177/2472630318760745.

[40] Z. Li, S. Han, X. Wang, F. Han, X. Zhu, Z. Zheng, H. Wang, Q. Zhou, Y. Wang, L. Su, J. Shi, C. Tang, D. Hu, Rho kinase inhibitor Y-27632 promotes the differentiation of human bone marrow mesenchymal stem cells into keratinocyte-like cells in xeno-free conditioned medium, Stem Cell Res. Ther. 6 (2015) 1–13, https://doi.org/10.1186/s13287-015-0008-2.

[41] M. Maldonado, R.J. Luu, M.E.P. Ramos, J. Nam, ROCK inhibitor primes human induced pluripotent stem cells to selectively differentiate towards mesendodermal lineage via epithelial-mesenchymal transition-like modulation, Stem Cell Res. 17 (2016) 222–227, https://doi.org/10.1016/j.scr.2016.07.009.

[42] M.A. Rasmussen, B. Holst, Z. Tümer, M.G. Johnsen, S. Zhou, T.C. Stummann, P. Hyttel, C. Clausen, Transient p53 suppression increases reprogramming of human fibroblasts without affecting apoptosis and DNA damage, Stem Cell Rep. 3 (2014) 404–413, https://doi.org/10.1016/j.stemcr.2014.07.006.

[43] B. Schmid, B. Holst, U. Poulsen, I. Jørring, C. Clausen, M. Rasmussen, U.A. Mau-Holzmann, R. Steeg, H. Nuthall, A. Ebneth, A. Cabrera-Socorro, Generation of two gene edited iPSC-lines carrying a DOX-inducible NGN2 expression cassette with and without GFP in the AAVS1 locus, Stem Cell Res. 52 (2021), https://doi.org/10.1016/j.scr.2021.102240.

[44] S. Altmaier, I. Meiser, E. Lemesre, B. Chanrion, R. Steeg, L.E. Leonte, B. Holst, B. S. Nielsen, C. Clausen, K. Schmidt, A.M. Vinggaard, H. Zimmermann, J. C. Neubauer, M.A. Rasmussen, Human iPSC-derived hepatocytes in 2D and 3D suspension culture for cryopreservation and in vitro toxicity studies, Reproductive Toxicology (2022), https://doi.org/10.1016/j.reprotox.2022.05.005.

[45] P.Y. Shih, M. Kreir, D. Kumar, F. Seibt, F. Pestana, B. Schmid, B. Holst, C. Clausen, R. Steeg, B. Fischer, J. Pita-Almenar, A. Ebneth, A. Cabrera-Socorro, Development of a fully human assay combining NGN2-inducible neurons co-cultured with iPSC-derived astrocytes amenable for electrophysiological studies, Stem Cell Res. 54 (2021), https://doi.org/10.1016/j.scr.2021.102386.

[46] M. Zhang, J.S. Schulte, A. Heinick, I. Piccini, J. Rao, R. Quaranta, D. Zeuschner, D. Malan, K.P. Kim, A. Röpke, P. Sasse, M. Araúzo-Bravo, G. Seebohm, H. Schöler, L. Fabritz, P. Kirchhof, F.U. Müller, B. Greber, Universal cardiac induction of human pluripotent stem cells in two and three-dimensional formats: Implications for in vitro maturation, Stem Cells 33 (2015) 1456–1469, https://doi.org/10.1002/stem.1964.

[47] B. Fischer, A. Meier, A. Dehne, A. Salhotra, T.A. Tran, S. Neumann, K. Schmidt, I. Meiser, J.C. Neubauer, H. Zimmermann, L. Gentile, A complete workflow for the differentiation and the dissociation of hiPSC-derived cardiospheres, Stem Cell Res. 32 (2018) 65–72, https://doi.org/10.1016/j.scr.2018.08.015.

[48] A. Rezania, J.E. Bruin, P. Arora, A. Rubin, I. Batushansky, A. Asadi, S. O'Dwyer, N. Quiskamp, M. Mojibian, T. Albrecht, Y.H.C. Yang, J.D. Johnson, T.J. Kieffer, Reversal of diabetes with insulin-producing cells derived in vitro from human pluripotent stem cells, Nat. Biotechnol. 32 (2014) 1121–1133, https://doi.org/10.1038/nbt.3033.

[49] A. Carpentier, I. Nimgaonkar, V. Chu, Y. Xia, Z. Hu, T.J. Liang, Hepatic differentiation of human pluripotent stem cells in miniaturized format suitable for high-throughput screen, Stem Cell Res. 16 (2016) 640–650, https://doi.org/10.1016/j.scr.2016.03.009.

[50] G. Pettinato, S. Lehoux, R. Ramanathan, M.M. Salem, L.X. He, O. Muse, R. Flaumenhaft, M.T. Thompson, E.A. Rouse, R.D. Cummings, X. Wen, R.A. Fisher, Generation of fully functional hepatocyte-like organoids from human induced pluripotent stem cells mixed with Endothelial Cells, Sci. Rep. 9 (2019) 1–21, https://doi.org/10.1038/s41598-019-45514-3.

[51] Y. Shi, P. Kirwan, F.J. Livesey, Directed differentiation of human pluripotent stem cells to cerebral cortex neurons and neural networks, Nat. Protoc. 7 (2012) 1836–1846, https://doi.org/10.1038/nprot.2012.116.

[52] P. Reinhardt, M. Glatza, K. Hemmer, Y. Tsytsyura, C.S. Thiel, S. Höing, S. Moritz, J. A. Parga, L. Wagner, J.M. Bruder, G. Wu, B. Schmid, A. Röpke, J. Klingauf, J. C. Schwamborn, T. Gasser, H.R. Schöler, J. Sterneckert, Derivation and expansion using only small molecules of human neural progenitors for neurodegenerative disease modeling, PLoS One 8 (2013), e59252, https://doi.org/10.1371/journal.pone.0059252.

[53] S.M. Chambers, C.A. Fasano, E.P. Papapetrou, M. Tomishima, M. Sadelain, L. Studer, Highly efficient neural conversion of human ES and iPS cells by dual inhibition of SMAD signaling, Nat. Biotechnol. 27 (2009) 275–280, https://doi.org/10.1038/nbt.1529.

[54] K. Blinova, J. Stohlman, J. Vicente, D. Chan, L. Johannesen, M.P. Hortigon-Vinagre, V. Zamora, G. Smith, W.J. Crumb, L. Pang, B. Lyn-Cook, J. Ross, M. Brock, S. Chvatal, D. Millard, L. Galeotti, N. Stockbridge, D.G. Strauss, Comprehensive translational assessment of human-induced pluripotent stem cell derived cardiomyocytes for evaluating drug-induced arrhythmias, Toxicol. Sci. 155 (2017) 234–247, https://doi.org/10.1093/TOXSCI/KFW200.

[55] S.P. Harrison, S.F. Baumgarten, R. Verma, O. Lunov, A. Dejneka, G.J. Sullivan, Liver organoids: recent developments, limitations and potential, Front. Med. 8 (2021) 534, https://doi.org/10.3389/FMED.2021.574047.